Arch. Mech., 40, 1, pp. 25–34, Warszawa 1988

Crystallographic analysis of shear bands initiation and propagation in pure metals
Part I. Initiation of shear bands in pure ductile single crystals

PH. DUBOIS, M. GASPERINI, C. REY and A. ZAOUI (VILLATANEUSE)

THE PAPER deals with the problem of verification of the theoretical model of shear band initiation in pure FCC-crystals proposed by Pierce. Experimental results of tension tests performed on copper single crystals are discussed. The results do not comply with the theoretical predictions of Pierce's model; the authors suggest the necessity of accounting for the effects of nonhomogeneous deformation and local elastic spin.

Praca poświęcona jest weryfikacji teoretycznego modelu procesu powstawania pasm ścinania w kryształach o regularnej sieci płasko-centrycznej, zaproponowanego przez Pierce'a. Omówiono wyniki badań doświadczalnych dotyczących prób rozciągania monokryształów miedzi. Autorzy dyskutują przyczyny niezgodności wyników tych badań z przewidywaniami teoretycznymi modelu Pierce'a sugerując konieczność uwzględnienia niejednorodności deformacji i lokalnego spinu sprężystego.

Работа посвящена проверке теоретической модели процесса возникновения полос сдвига в кристаллах с регулярной плоско-центрированной решеткой, предложенной Пирсом. Обсуждены результаты экспериментальных исследований, касающихся испытаний растяжения монокристаллов меди. Авторы обсуждают причины несовпадения результатов этих исследований с теоретическими предсказываниями модели Пирса, предполагая необходимость учета неоднородности деформации и локального упругого спина.

1. Introduction

OUR PURPOSE was to perform tensile tests on differently oriented pure copper single crystals in order to determine the nature of the resulting shear planes and to compare our experimental results with the predictions of theoretical models. First, a summary of previous work is proposed.

At the beginning of tensile straining, single crystals of ductile pure metals exhibit at a macroscopical scale a homogeneous deformation according to one or two slip systems. With increasing loading, the homogeneous deformation turns to a heterogeneous one through the onset of diffuse necking and, for well-defined tensile axis orientation, localized shearing. In the latter case, failure occurs by crack formation inside intense shear bands.

In fcc single crystals, the formation of shear bands was observed for double slip orientations [1]. This means that the orientation of the tensile axis was situated in a (110) plane; thus the activated slip systems were the primary and the conjugate ones. They strongly interacted and probably built up Lomer Cottrell locks. In pure metals, the observed shear planes were generally close to crystallographic planes, and different situations, depending on the tensile axis orientations, were especially studied: for a tensile axis parallel to the

[111] direction, only one kind of shear bands characterized by a (100) shear plane and constituted by stretched cells of dislocations could be observed [2, 3]. But for a tensile axis parallel to the [112] direction, two kinds of shear bands characterized by shear planes parallel to the primary and conjugate planes, respectively, were activated.

Some other phenomena were pointed out: the shear bands are harder than the bulk and present large lattice rotations [2].

Latent hardening properties of the involved metals play a major part in the determination of the threshold strain corresponding to the onset of shear bands and in the shear density [1, 4]. The threshold strain increases with increasing stacking fault energy whereas the amount of shear bands decreases. Though it is more difficult to obtain shear bands in pure metals as compared with alloys, the shear band onset conditions are easier to analyse in the former ones.

On a theoretical view point many previous works [5, 6] attempted to perform quantitative analyses of shear bands formation using continuum mechanics. The major difficulties connected with describing of the constitutive equations able to characterize the plastic flow at finite strains. Founding upon HILL and HUTCHINSON [5] and BIOT'S works [7] and taking into account crystallographical considerations, an analysis of the conditions of shear bands onset in an idealized isotropic incompressible two-dimensional single crystal undergoing a symmetric double slip deformation was proposed [8, 9]. These conditions depend upon the deformation kinematics of the crystal and could be expressed as functions of latent hardening parameters of the relevant metal.

A three-dimensional model of shear bands bifurcation was developed by PIERCE [10] for fcc ductile crystals. The crystal plasticity was assumed to be rate-independent and to be governed by a crystallographic slip according to Schmid's law. It was also assumed that the crystal was undergoing a double slip deformation under tensile loading. For such a double slip orientation, a thin band of intense shearing limited by two nearly parallel shear planes grew in the crystal.

The transformation gradient rate $\mathring{\mathbf{F}}$ showed an abrupt change of value in the thin band by comparison to the bulk, the deformation gradient tensor $\mathbf{F}$ being continuous.

According to Pierce, the discontinuity $\Delta\mathring{\mathbf{F}}$ must be of the form:

$$\Delta\mathring{\mathbf{F}} = \mathbf{G}\times\mathbf{N}, \tag{1.1}_1$$

$\mathbf{G}$ is the shearing vector and $\mathbf{N}$ is the unit normal to the band in the reference configuration (undeformed configuration).

Traction rates must be continuous across the shear plane, so one must have

$$\mathbf{N}\cdot\Delta\mathring{\mathbf{S}} = 0, \tag{1.1}_2$$

$\mathbf{S}$ is the nominal stress defined so that $\mathbf{N}\cdot\mathbf{S}$ is the force per unit reference area on the plane whose unit normal was $\mathbf{N}$ in the reference configuration.

The discontinuity of the total stretching rate $\Delta\mathbf{D}$ is given by

$$\Delta\mathbf{D} = \frac{1}{2}(\mathbf{g}\times\mathbf{n}+\mathbf{n}\times\mathbf{g}), \tag{1.2}$$

where $\mathbf{n}$ and $\mathbf{g}$ are defined in the current configuration by

$$\mathbf{n} = \mathbf{N}\cdot\mathbf{F}^{-1}/|\mathbf{N}\cdot\mathbf{F}^{-1}| \quad \text{and} \quad \mathbf{g} = \mathbf{G}|\mathbf{N}\cdot\mathbf{F}^{-1}|. \tag{1.3}$$

In the case of a rigid plastic behaviour we can write

$$\Delta\mathbf{D} = \sum_i \mathbf{P}^{(i)} \Delta\dot{\gamma}^{(i)} \tag{1.4}$$

with

$$\mathbf{P}^{(i)} = \frac{1}{2}(\mathbf{s}^{*(i)} \times \mathbf{m}^{*(i)} + \mathbf{m}^{*(i)} \times \mathbf{s}^{*(i)});$$

$\mathbf{s}^{*(i)}$ is a vector parallel to the slip direction of the (i) active slip system; $\mathbf{m}^{*(i)}$ is a vector normal to the (i) slip plane; $\mathbf{s}^{*(i)}$ and $\mathbf{m}^{*(i)}$ are given in the current configuration; $\Delta\dot{\gamma}^{(i)}$ is the discontinuity of the slipping rate on the relevant (i) slip system.

The knowledge of the nature of the two activated slip systems (hereafter named (1.1) and (1.2)) and of $\Delta\dot{\gamma}^{(1)}$ and $\Delta\dot{\gamma}^{(2)}$ values allow to determine $\mathbf{g}$ and $\mathbf{n}$ from Eqs. (1.2) and (1.4).

This calculation is valid at the onset of shear bands but cannot describe the propagation. More details are given in the discussion.

After some calculations, Pierce showed that the localization was possible if the following equation is satisfied:

$$\Delta\overset{\nabla}{\boldsymbol{\tau}} : \Delta\mathbf{D} = \frac{1}{2}|\mathbf{g}\cdot\boldsymbol{\tau}\cdot\mathbf{g} - \mathbf{g}\cdot\mathbf{g}(\mathbf{n}\cdot\boldsymbol{\tau}\cdot\mathbf{n})|, \tag{1.5}$$

where $\overset{\nabla}{\boldsymbol{\tau}}$ is the Jaumann derivative of the Kirchhoff stress $\boldsymbol{\tau}$ based on the material rotations and $\Delta\boldsymbol{\tau}$ is the discontinuity of $\boldsymbol{\tau}$ across the interface which separates the matrix and the shear band.

$\Delta\overset{\nabla}{\boldsymbol{\tau}} : \Delta\mathbf{D}$ could be written as a function of H^{ij} using

$$\mathbf{P}^{(i)} : \overset{\nabla}{\boldsymbol{\tau}} = \sum_j H^{ij}\dot{\gamma}^{(j)} \tag{1.6}$$

with

$$H^{ij} = h^{ij} - P^{(i)} : \beta^{(j)}; \tag{1.7}$$

h^{ij} is the hardening matrix of the relevant metal.

$$\boldsymbol{\beta}^{(j)} = \mathbf{W}^{(j)}\cdot\boldsymbol{\tau} - \boldsymbol{\tau}\cdot\mathbf{W}^{(j)} \quad \text{and} \quad \mathbf{W}^{(j)} = \frac{1}{2}(\mathbf{s}^{*(j)} \times \mathbf{m}^{*(j)} - \mathbf{m}^{*(j)} \times \mathbf{s}^{*(j)}).$$

2. Experimental procedure

Single crystals were obtained from initially 99.5% pure copper thanks to the Bridgman vertical growth method under secondary vacuum. The samples $15 \times 7 \times 2$ mm^3 were cut out by spark machining, then chemically polished. The specimen orientations were checked using the backwards Laue technique.

Tensile tests were performed at room temperature, the strain rate was about 10^{-4} s^{-1}. Observations were carried out at different stages of the plastic strain through a SEM (the depth of field of SEM allowing observations of wavy surfaces such as necking areas).

3. Experimental results

Three orientations of the tensile axis, respectively close to the [$\bar{1}11$], [001] and [$\bar{1}12$] crystallographic directions of the single crystals, were investigated. In the three cases, the samples were in double slip orientation, the two observed slip systems being the primary and the conjugate ones, named hereafter B_4 and C_1, respectively, in the Schmid and Boas notation.

Shear bands became visible at a macroscopic strain of about 55% and were localized in the necking area but differences upon their crystallographical nature could be pointed out as a function of the tensile axis orientation.

3.1. Quasi [111] orientation

The Schmid factors on B_4 and C_1 slip systems were equal to 0.31 and 0.29, respectively. The resulting slip pattern was heterogeneous: the B and C planes were activated in adjacent areas and did not intersect each other except in the necking area.

The onset of two shear bands in the necking area was observed at about 60%; they were parallel to the B and C planes, respectively, and gave rise to a crack at their intersection. A sketch of the slip pattern is given in Fig. 1.

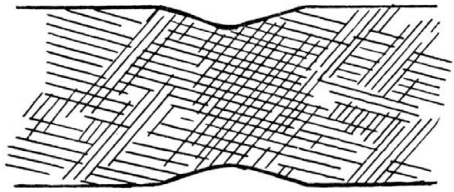

FIG. 1. Sketch of the slip pattern of a [111] tensile tested single crystal.

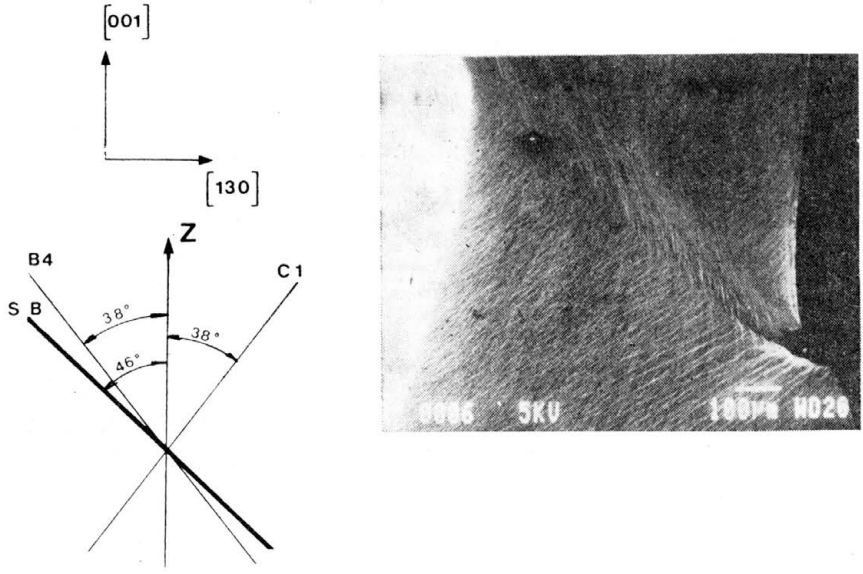

FIG. 2. Shear band in [001] oriented copper single crysta

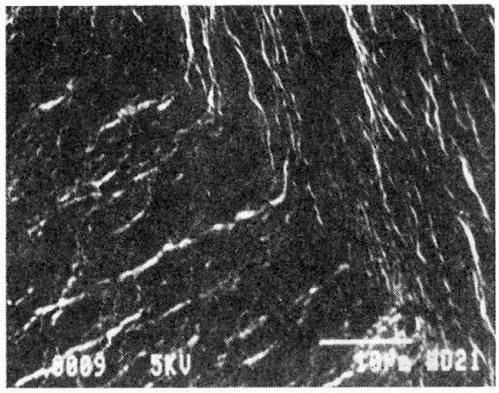

FIG. 3. Detail of shear band in the [001] oriented single crystal.

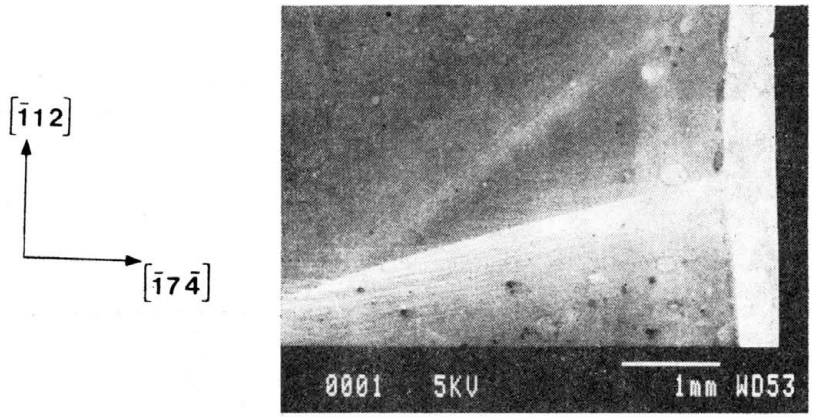

(a)

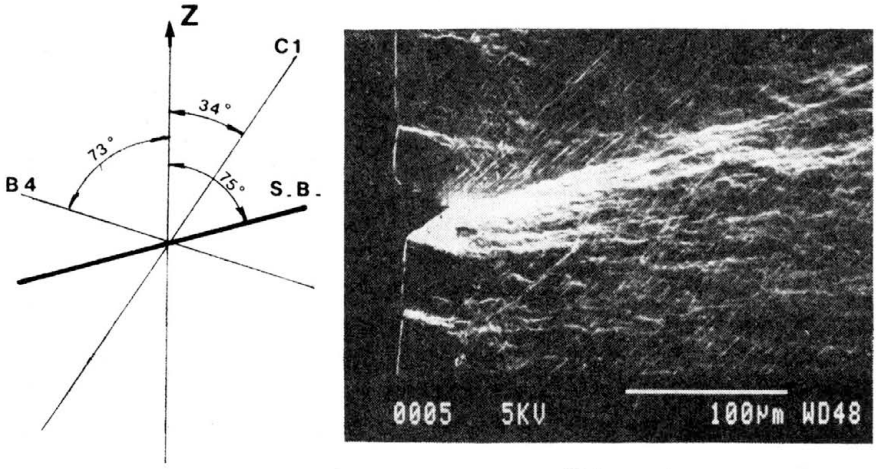

(b)

FIG. 4. a) Shear band on the large face of a [$\bar{1}$12] tensile tested copper single crystal. b) Details of the slip bands around the shear band.

3.2. Quasi [001] orientation

The Schmid factors on B_4 and C_1 slip systems were equal to 0.42 and 0.40, respectively. The resulting slip pattern was similar to the $[\bar{1}11]$ one: inhomogeneous in the whole sample except in the necking area. Only one shear band parallel to a $(\bar{1}01)$ plane was observed (Fig. 2). Inside the shear band, the activation of the primary slip system (B_4) seemed higher than the secondary (C_1) one.

In Fig. 3, the shear band plane is clearly visible as well as the variation of the amount of activity of B_4 and C_1 on each side of the shear band plane.

Moreover, the misorientation of the B plane marks outside and inside the shear band was about 10 degrees and pointed out the existence of a lattice rotation inside the band.

All these observations led to consider that the shear band formation induces a discontinuity of the amount of crystallographic shear $\Delta\gamma$ on B_4 and C_1.

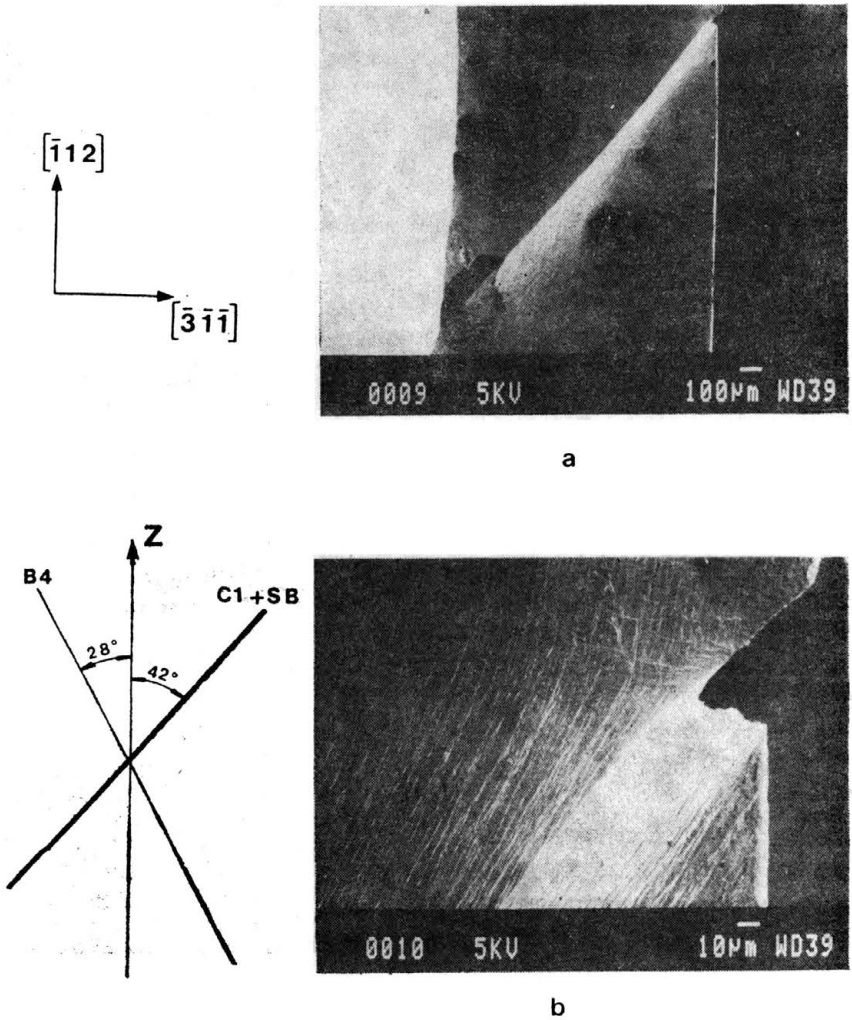

FIG. 5. a) Shear band on the (311) face of a $\bar{1}$[112] tensile tested copper single crystal. b) Details of the slip bands around the shear band.

3.3. $[\bar{1}12]$ orientation

The B_4 and C_1 slip systems had the same Schmid factors, equal to 0.42 and were simultaneously activated. In this case of accurate symmetry, the sample exhibited an homogeneous slip pattern. A single shear band parallel to a (112) plane appeared in the necking area as soon as the reduction of section reached 10%. Cracks were observed at the surface sample in the shear band.

Microphotographies of the two perpendicular faces of the sample are given in Figs. 4a and 5a. Details of slip systems inside and outside the shear band can be seen in Figs. 4b and 5b. After shearing, we observed a high activity of the B_4 slip system in the shear band.

4. Discussion

According to PIERCE [10], a limited collection of shearing modes can exist in a rigid plastic fcc crystal restricted to slip on a primary and conjugate pair of slip systems. Using Eqs. (1.2) and (1.4) with

$$\mathbf{s}^{*(1)} = \frac{1}{\sqrt{2}}[\bar{1}01], \quad \mathbf{m}^{*(1)} = \frac{1}{\sqrt{3}}(111),$$

$$\mathbf{s}^{*(2)} = \frac{1}{\sqrt{2}}[011], \quad \mathbf{m}^{*(2)} = \frac{1}{\sqrt{3}}(\bar{1}\bar{1}1),$$

we derive the possible solutions:

mode	**g**	**n**	$\Delta\mathring{\gamma}^{(1)}$,	$\Delta\mathring{\gamma}^{(2)}$
1	$\lambda[\bar{1}11]/\sqrt{3}$	$(110)/\sqrt{2}$	$\Delta\mathring{\gamma}^{(1)} =$	$-\Delta\mathring{\gamma}^{(2)} = \lambda$
2	$\lambda[110]/\sqrt{2}$	$(\bar{1}11)/\sqrt{3}$	$\Delta\mathring{\gamma}^{(1)} =$	$-\Delta\mathring{\gamma}^{(2)} = \lambda$
3	$\lambda[111]/\sqrt{3}$	$(\bar{1}01)/\sqrt{2}$	$\Delta\mathring{\gamma}^{(1)} = \lambda$	$\Delta\mathring{\gamma}^{(2)} = 0$
4	$\lambda[111]/\sqrt{2}$	$(111)/\sqrt{3}$	$\Delta\mathring{\gamma}^{(1)} = \lambda$	$\Delta\mathring{\gamma}^{(2)} = 0$
5	$\lambda[\bar{1}\bar{1}1]/\sqrt{3}$	$(011)/\sqrt{2}$	$\Delta\mathring{\gamma}^{(1)} = 0$	$\Delta\mathring{\gamma}^{(2)} = -\lambda$
6	$\lambda[011]/\sqrt{2}$	$(\bar{1}\bar{1}1)/\sqrt{2}$	$\Delta\mathring{\gamma}^{(1)} = 0$	$\Delta\mathring{\gamma}^{(2)} = -\lambda$

g and **n** are given by the formulae (1.3), **n** is a unit vector defined in the current configuration, **g** is proportional to the shearing vector **G** in the underformed configuration: $\mathbf{g} = \lambda\mathbf{G}$; $|\mathbf{g}| = \lambda$.

In the case of a rigid plastic behaviour, the current configuration can be deduced from the relaxed configuration by a rigid body rotation of the crystal.

These results are similar to Pierce's ones, which were obtained for a different orientation but for an equivalent symmetry of the activated slip systems.

Let us consider the six calculated modes. According to Pierce, modes 1 and 2 were not admissible in that they involved unloading on one of the already active slip systems ($\Delta\mathring{\gamma}^{(1)} = -\Delta\mathring{\gamma}^{(2)}$).

The other modes involve a discontinuity of the amount of shearing only on one slip system. The relevant bifurcation planes corresponded to "kink planes" (modes 3 and 5) and to activated slip planes (modes 4 and 6). These six planes were well known as compatible interfaces able to separate, in a single crystal or in a grain of a polycrystal, areas deformed according to only one slip system (here B_4 or C_1) without inducing internal stresses. These planes could be easily deduced from the compatibility equations [11] written in the rigid plastic case, i.e. without any elastic accommodation. Therefore, such a calculation was unable to forecast (112) localization planes. On the other hand, the localization planes and the discontinuity $\Delta\mathring{\gamma}^{(i)}$ on slip systems (i) given by modes 4 and 6 fitted our observations 3a and 3b.

Now, let us write the localization conditions. According to Pierce, localization is possible if the equality (1.5) is verified for "reasonable" values of $(h/\sigma)_c$ and q where σ is the tensile component, h corresponds to the diagonal components of the hardening matrix and $h' = qh$ corresponds to the nondiagonal ones. For current metals, the accepted values of q are such as $1 < q < 1.4$.

The calculation was carried out for a tensile axis **Z** belonging to the (110) plane and misoriented with regard to the [001] direction. For values of **g**, **n**, $\Delta\mathring{\gamma}^{(1)}$ and $\Delta\mathring{\gamma}^{(2)}$ reported in the hereabove table we obtained:

(4.1) mode 1 $$(h/\sigma)_c = -\frac{1+\sqrt{2}\,\sin 2\alpha+\cos 2\alpha}{12(q-1)},$$

(4.2) mode 2 $$(h/\sigma)_c = -\frac{4+3\sqrt{2}\,\sin 2\alpha}{12(q-1)},$$

(4.3) modes 4 and 6 $$(h/\sigma)_c = 0,$$

(4.4) modes 3 and 5 $$(h/\sigma)_c = \frac{2+3\sqrt{2}\,\sin 2\alpha+\sin 2\alpha}{12},$$

α is the angle between **Z** and [001]; its values depend on the **Z** chosen orientation.

No noticeable variation of $(h/\sigma)_c$ with increasing α ($0 < \alpha < 52°$) was obtained. The localization can occur if the ratio $(h/\sigma)_c$ is positive and not too small. Unfortunately, such a situation corresponded to modes 1 and 2 which were not physically admissible.

In the four other cases which corresponded to observed phenomena, $(h/\sigma)_c$ was equal to zero (modes 4 and 6) or negative (modes 3 and 5): no bifurcation was possible.

Let us focus on the localization process on the plane (112). In order to solve Eq. (1.5), we chose to estimate $\Delta\mathring{\gamma}^{(1)}$ and $\Delta\mathring{\gamma}^{(2)}$ through a method different from Pierce's one and based on KRÖNER's theory of incompatibility [11]. We assumed that the incompatible plastic deformation due to the discontinuity on $\Delta\mathring{\gamma}^{(1)}$ and (or) $\Delta\mathring{\gamma}^{(2)}$ across the (112) interface could be accommodated by elastic strains which induced internal stresses in the

crystal. It could be shown that the lowest calculated internal stresses corresponded to the case where only the B_4 slip system had a slipping rate discontinuity (i.e. $\Delta\mathring{\gamma}^{(1)} = \lambda$ and $\Delta\mathring{\gamma}^{(2)} = 0$).

Physical considerations helped us to estimate g:g has to be at the same time in the shear plane (112) and in the plane $(1\bar{1}1)$ which contains the two directions $\mathbf{s}^{*(1)}$ and $\mathbf{s}^{*(2)}$; $\mathbf{g} = \frac{\lambda}{\sqrt{14}}[31\bar{2}]$ proved to be an admissible solution.

For $\Delta\mathring{\gamma}^{(1)} = \lambda$, $\Delta\mathring{\gamma}^{(2)} = 0$ and $g = \frac{\lambda}{\sqrt{14}}[31\bar{2}]$, one obtains from equation (1.5):

$$(h/\sigma)_c = -\frac{1}{12}(2+\sqrt{2}\sin 2\alpha+\sin^2\alpha), \tag{4.5}$$

$(h/\sigma)_c$ is also negative and localization is theoretically impossible.

The conclusion is then that there is a misfit between the experimental observations and Pierce's model forecasting.

The assumption of the rigid plastic behaviour does not play the most important role in the misfit: to take into account the elastic rate of stretching does not really improve the $(h/\sigma)_c$ values in the three-dimensional case.

In order to improve the theoretical model, many other assumptions need to be cleared up:

The first point is concerned with the Schmid law derivation. Pierce assumed that $\mathbf{s}^{*(i)}$ and $\mathbf{m}^{*(i)}$ vectors were the same in both reference and relaxed configurations. If these two vectors are considered as material vectors, the bifurcation criterion may be modified.

Two other points must be investigated:

Before the onset of the shear bands the deformation according to symmetrical slip systems with regard to the tensile axis was assumed to be homogeneous and, consequently, no elastic spin was possible. We have to keep in mind that the observed heterogeneous deformation with possibilities of local elastic spin may play an important part on the localization conditions.

The shear bands appear in the necking area which can be hardly described by a uniaxial tensile stress. A planar stress tensor would seem more convenient. In this case, activation of a third slip system is possible and may induce a lattice rotation in the necking zone.

Our purpose is now to take into account these three points in the model.

References

1. Y. W. CHANG and R. J. ASARO, Acta Met., **29**, 241, 1980.
2. S. SAIMOTO *et al.*, Phil. Mag., **21**, 319, 1965.
3. Z. JAZIENSKI, ICSMA, 4, 1, 75, 1976.
4. R. J. PRICE and A. KELLY, Acta Met., **12**, 979, 1964.
5. R. HILL and J. W. HUTCHINSON, J. Mech. Phys. Solids, **23**, 239, 1975.
6. V. TVERGAARD *et al.*, J. Mech. Phys. Solids, **29**, 115, 1981.
7. M. A. BIOT, *Mechanics of incremental deformations*, ed. by Willey, 1965.
8. R. J. ASARO, Acta Met., **27**, 445, 1979.

9. D. PIERCE *et al.*, Acta Met., **30**, 1087, 1982.
10. D. PIERCE, J. Mech. Phys. Solids, **31**, 133, 1983.
11. E. KRÖNER, *Dislocation field theory*, Summer School of Krazany, 231, 1964.

LABORATOIRE PMTM DU CNRS
UNIVERSITÉ PARIS-NORD, VILLETANEUSE, FRANCE.

Received January 2, 1987.